Structural and morphological studies of Nd-doped phosphate thin films deposited by PLD on silicon wafers

C. R. IORDANESCU[a], I. D. FERARU[a,*], M. ELISA[a], I. C. VASILIU[a], A. VOLCEANOV[b], S. STOLERIU[b], M. FILIPESCU[c]
[a]*National Institute of R & D for Optoelectronics INOE 2000, 409 Atomistilor Str., Magurele RO-077125, Romania*
[b]*Faculty of Applied Chemistry and Materials Science, 1 Polizu Str., Bucharest, Romania*
[c]*National Institute for Laser, Plasma and Radiation Physics, Magurele, Romania*

Nd-doped phosphate thin films were obtained by pulsed laser deposition (PLD) technique on silicon wafers using a Nd-doped $Li_2O–BaO–Al_2O_3–La_2O_3–P_2O_5$ bulk target. An excimer laser with 248 nm wavelength was used to ablate the vitreous doped phosphate glass. The oxygen pressure and the substrate temperature were varied during the deposition process as follows: a) high vacuum (3×10^{-6} Torr) and T_s = 20 °C; b) $P_{O\,2}$= 1.5×10^{-3} Torr and T_s = 20 °C; c) high vacuum and T_s = 400 °C and d) P_{O2} = 1.5×10^{-3} Torr and T_s=400 °C. It was investigated the influence of these parameters on the compactness and uniformity of the films. The structural characterization of the films was performed using micro-Raman spectroscopy and Fourier Transform Infrared spectroscopy (FTIR). The chemical characterization and the morphology of the films were made by Energy Dispersive X-ray spectroscopy (EDX), Scanning Electron Microscopy (SEM) and Atomic Force Microscopy (AFM). It was noticed that the specific molecular vibrations of the ablated target were reproduced in the fabricated PLD films. The obtained films show good uniformity and well preserved stoichiometry.

(Received December 15, 2013; accepted March 13, 2014)

Keywords: Phosphate glass, Rare-earth, Pulsed laser deposition, Raman spectroscopy, FTIR spectroscopy, SEM-EDX analysis

1. Introduction

Phosphate glasses studied in the last decades present a variety of technological and optical applications due to their specific properties [1-3]. Glasses based on P_2O_5 are good host materials for rare-earth ions and suitable to be used as photonic devices such as high power lasers, fiber and waveguide amplifiers, optical isolators, photosensitivity based devices, scintillators and optical storage device [4-7].

Amorphous materials based on phosphate glasses doped with rare-earth elements (RE) have been intensively studied in the recent decades because they are important components of a new generation of multimedia systems [8-12]. Laser glasses are able to be cast into a variety of forms and sizes with excellent homogeneity uniformly distributed doping ion concentrations, and relatively low cost [13]. Along with bulk laser glasses, film/substrate composite structures are being studied. In these structures, un-doped or RE-doped silicate-phosphate films are deposited on various substrates (glass, ITO/glass, Si) [12]. Nd-doped phosphate glasses have been widely used in high average power laser solid state lasers, laser material processing, range finder and other industrial and scientific applications. Thin phosphate films containing neodymium ions (Nd^{3+}) are used as active elements in planar optical waveguides, integrated lasers, amplifiers, etc. Generally, they are superior to silicate films in their optical characteristics but inferior in their strength properties [14-16].

Pulsed laser deposition (PLD) is a recently developed technique which is compatible with deposition in gas environments and has been applied successfully to grow a wide variety of multicomponent materials in thin film configuration. It has been shown to be especially suited for the development of films for optical applications [17]. The deposition of planar waveguides by PLD has been demonstrated, and most of the effort has been focused on achieving films of good epitaxial quality [18]. A major problem in PLD of phosphate glasses is the low quality of thin film surfaces that are covered by droplets and by fragments ejected from the glass target [19, 20]. Even when short laser wavelengths (266 or 248 nm) are used for ablation or when deposition is performed in off-axis configurations, the thin films exhibit surface roughness of hundreds of nm up to few micrometers [21].

In spite of the advantages of glasses for developing active waveguides, and although the growth of multicomponent oxides by PLD appears to be the most successful route, the number of studies devoted to the production of glassy films by PLD has been limited [22-24]. It is well known that the P_{O2} in the chamber is one of the most critical parameters for the PLD of complex oxide films. It has been shown earlier that amorphous semiconductor films grown by PLD are denser than those grown with other deposition techniques due to the presence of energetic species during the PLD process [25]. Moreover, studies of the plume expansion during PLD of complex oxide films have shown that P_{O2} has a significant effect on the kinetic energy of the species ablated from the

target [26] the higher the P_{O2} the lower the kinetic energy of the expelled material particles.

This work presents a structural and morphological study on glassy thin films deposited on silicon substrates by pulsed laser deposition. Due to high solubility of rare-earth ions in the phosphate glasses, it is possible to deposit thin films with high Nd ion concentration from a bulk phosphate glass. PLD technique allows preparing thin films with chemical composition close to that of the bulk glass target, suited to high bandwidth fully integrated waveguide devices.

2. Experimental

Ablation and deposition processes were performed in a stainless steel vacuum chamber. A pulsed KrF excimer laser (CompexPro 201-Coherent) operating at 248 nm, with a repetition rate of 10 Hz and pulse width of 20 ns, was used as source for the ablation process. After having been reflected on two high-energy laser mirrors, the laser beam enters the stainless steel vacuum chamber through a quartz window and it is focused through a focal lens on a rotating target under an incidence angle of 60°, providing a rectangular profile of the laser spot at the target impact. The substrate is positioned parallel to the target at a distance of 60 mm. The deposition chamber was pumped at a pressure of about 10^{-7} mbar before and after starting the deposition process. As target, Nd^{3+}-doped Li_2O–BaO–Al_2O_3–La_2O_3–P_2O_5 glass have been prepared using Li_2CO_3, $BaCO_3$, Al_2O_3, La_2O_3, H_3PO_4 and Nd_2O_3 as analytical grade reagents. The starting batch composition corresponds to the molar formula: 56.67 $LiPO_3$, 28.33 $Al(PO_3)_3$, 10 $Ba(PO_3)_2$, 2 La_2O_3, 3 Nd_2O_3 and to the following oxide composition (wt. %): 4.27 Li_2O, 7.25 Al_2O_3, 7.68 BaO, 3.27 La_2O_3, 72.04 P_2O_5 and 5.51 Nd_2O_3. The reagents are introduced in H_3PO_4 solution at the very beginning of the starting process, under continuous stirring. The glass samples were melted at 1250 °C for 4 hours, in alumina crucibles and then annealed at 450 °C for 6 hours. The improvement of glass melt optical quality was performed by using a special mechanical stirring device, provided with an alumina stirrer. The rotation speed was varied between 100 and 250 rot/min, in dependency on temperature and viscosity of the glass melt.

The films were deposited on substrates of n-type Si wafers with dimensions of 10/10 mm previously cleaned in HF 10 %, followed by distilled water and ethylic alcohol, quick-drying in air.

In order to improve the morphology of the films we performed a study varying two parameters: the pressure in the vacuum chamber and the Si substrate temperature, during the deposition process, as following in Table 1.

Table 1. The variation of parameters in the pulsed laser deposition processes.

No. exp.	Pressure (Torr)	Substrate temperature (°C)	Laser energy/pulse (mJ)
1	Vacuum (3×10^{-6})	Room temperature	450
2	Vacuum (3×10^{-6})	400	450
3	O_2 atmosphere ($1,5\times10^{-3}$)	Room temperature	450
4	O_2 atmosphere ($1,5\times10^{-3}$)	400	450
5	Vacuum (3×10^{-6})	Room temperature	350

UV-Vis absorbance spectrum was collected by using a Perkin Elmer Lambda 1050 spectrophotometer, in the range 300-650 nm.

Structural properties were provided by Raman and FTIR spectroscopy. Raman spectra were collected by means of LabRAM HR 800 UV-VIS-NIR Horiba Jobin-Yvon system, at room temperature. The samples were excited with the 633 nm line of He-Ne ion laser, focused on the surface sample with a confocal microscope, using an objective magnification ×100, 1 μm^2 laser spot size, laser power on the surface sample 2.8 mW, and 0.5 to 1 cm^{-1} resolution with an 1800 g/mm grating.

The Fourier Transform IR spectra were recorded with a Perkin Elmer Spectrophotometer-Spectrum 100, provided with UATR accessory (Universal Attenuated Total Reflectance) in the range 550-1500 cm^{-1}. The measurement error is ± 0.1 % and the number of scans 32.

For observing the morphology and the distribution of the elements in the films, Scanning Electron Microscopy (SEM) and Energy-dispersive X-ray (EDX) spectroscopy

investigations were performed with a SEM Hitachi S-2600N instrument.

The surface structure of Nd-doped phosphate glass was observed by Atomic Force Microscopy (AFM), namely AFM-XE 100 Park system.

3. Results and discussion

In the Fig. 1, the transmission (UV-Vis) spectrum of the Nd-glassy target is shown. The presence of Nd in the phosphate glass matrix is highlighted by the appearance of the specific absorption bands in visible domain (570-620 nm; 690-845 nm), in accordance with the data previously reported [27].

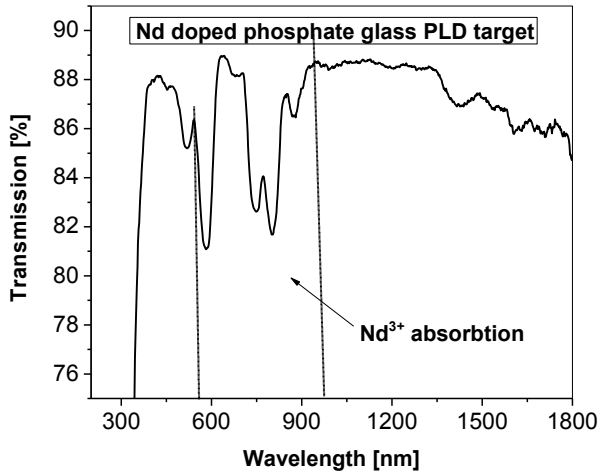

Fig. 1. The transmission spectrum of the Nd-doped phosphate glass plate, in the 200-1800 nm range.

Information about the structure of the aluminophosphate glasses doped with neodymium ions were provided firstly by micro-Raman spectroscopy. For comparison, the spectra of the target and of the silicon substrate are shown in the Fig. 2. The Raman data for all four experiments show signals from the glass matrix at about 350 cm^{-1}, 700 cm^{-1} and 1200 cm^{-1}, assigned to (O-P-O) bending, to (P-O-P) symmetrical stretching vibration mode and to (O-P-O) symmetrical non-bridging bond in Q^2 units, respectively [28-30]. These three peaks are found in the target and reproduced with weaker intensity in all the PLD films. The maximum around 1200 cm^{-1} is left shifted in the case of the films compared with the target, probably due to the stress resulted after the rearrangement of the glassy material on the silicon surface during the PLD process. Taking into account that alumina content in the glass target is lower than 10 mol. %, it is to be expected the lack of $(AlO_5)^{4-}$ tetrahedra in the glass network, as it was reported in [31].

Pumping oxygen in the vacuum chamber can induce a decreasing of the deposition rate, though the films from experiments 3 and 4 are thinner, as it can be seen in the Raman spectra, where the silicon vibrational mode appears at 520 cm^{-1} (the small thickness of the films allows the laser beam to penetrate the sample to the silicon substrate).

Raman peaks associated with silicon appear in the films from experiments 3, 4 and 5 due to the reduced thickness and low compactness of the deposited films.

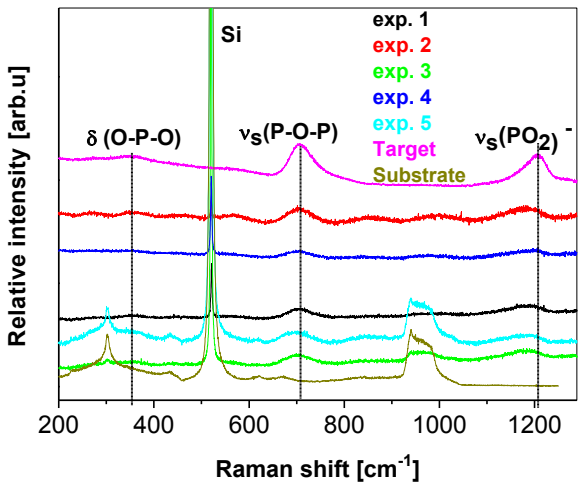

Fig. 2. Raman spectra provided with 633 nm laser excitation; δ - bending, ν_s - symmetric stretching.

As a complementary method related to the structural characterization of the studied samples the absorption spectra in the IR range were recorded (figure 3). We assigned the 1260 cm^{-1} peak to $(PO_2)^-$ asymmetrical stretch and/or to P=O stretch and the 1080 cm^{-1} peak is assigned to $(PO_3)^{2-}$ asymmetrical stretch and/or to PO_2 symmetrical stretch. The 787 cm^{-1} and 736 cm^{-1} peaks (the inset of the Fig. 3a) were obtained by the decomposing of a large IR absorption band (P-O-P symmetrical stretch) followed by the peak at about 905 cm^{-1} ($(PO_4)^{3-}$ asymmetrical stretch). The deposited films present a shift of IR peaks towards higher wave numbers compared with the target (especially for the vibrations of $(PO_4)^{3-}$ groups). We also observed an absorption band specific to hydrogen bonds with phosphorous network at 1499 cm^{-1} in case of the target, experiment 1 and 3, and the peak at 1644 cm^{-1} specific to O-H bend present only in the film from experiment 1 (no heat treatment and no oxygen pressure during the deposition).

The assignment of IR and Raman peaks are presented in the Table 2 and are in agreement with reference data [28-30, 32, 33].

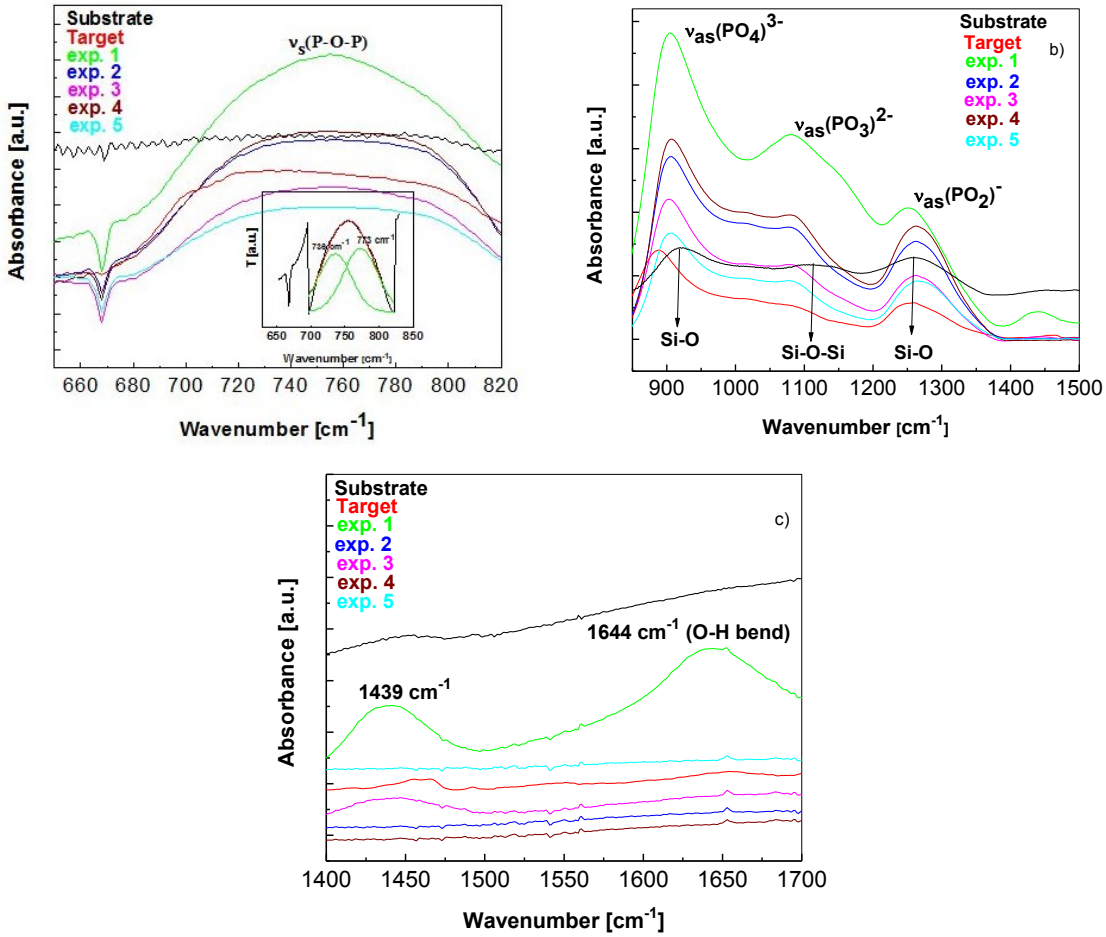

Fig. 3. FTIR-UATR spectra of Nd-doped phosphate glass films in the range a) 600-820 cm^{-1}; b) 850-1500 cm^{-1} and c) 1400-1700 cm^{-1}; ν_s - symmetric stretching vibration mode, ν_{as} - asymmetric stretching vibration mode.

Table 2. The corresponding Raman and IR vibrational modes for the Nd-doped phosphate glass films [33].

Wavenumber (cm^{-1})		Assignement
Raman	IR	
350	-	O-P-O bending
705	736	P-O-P symmetrical stretching
-	787	P-O-P symmetrical stretching
-	905	$(PO_4)^{3-}$ asymmetrical stretching
-	1080	$(PO_3)^{2-}$ asymmetrical stretching and/or to PO_2 symmetrical stretching
1200	-	$(PO_2)^{-}$ asymmetrical stretching
-	1260	$(PO_2)^{-}$ symmetrical stretching
-	1499	P-O-H stretching
-	1644	O-H bending

The morphology of thin films was firstly investigated by SEM. The images presented in Figs. 4a-d show the glassy film surfaces covered by specific PLD droplets with varying diameters between 1-5 μm. The highest compactness of the deposited Nd-doped film was obtained for the experiment 2. It seems that the substrate annealing and the high vacuum during the deposition process positively influence the uniformity and compactness of the films.

EDX investigation revealed elements like P, Al, Ba and La (forming elements of the bulk glassy matrix) for the vitreous film deposited on silicon substrate. In the Fig. 5a the EDX spectrum and the elemental mapping for the sample obtained in experiment 2 are presented. EDX mapping (Fig. 5b) sustains the presence of the constituent elements in the films reproduced from the target and their uniform distribution on the layer surface. Silicon line is noticed in EDX spectrum due to the substrate influence. Nd dopant can't be revealed by EDX measurement because of the device limiting regarding the rare-earth elements.

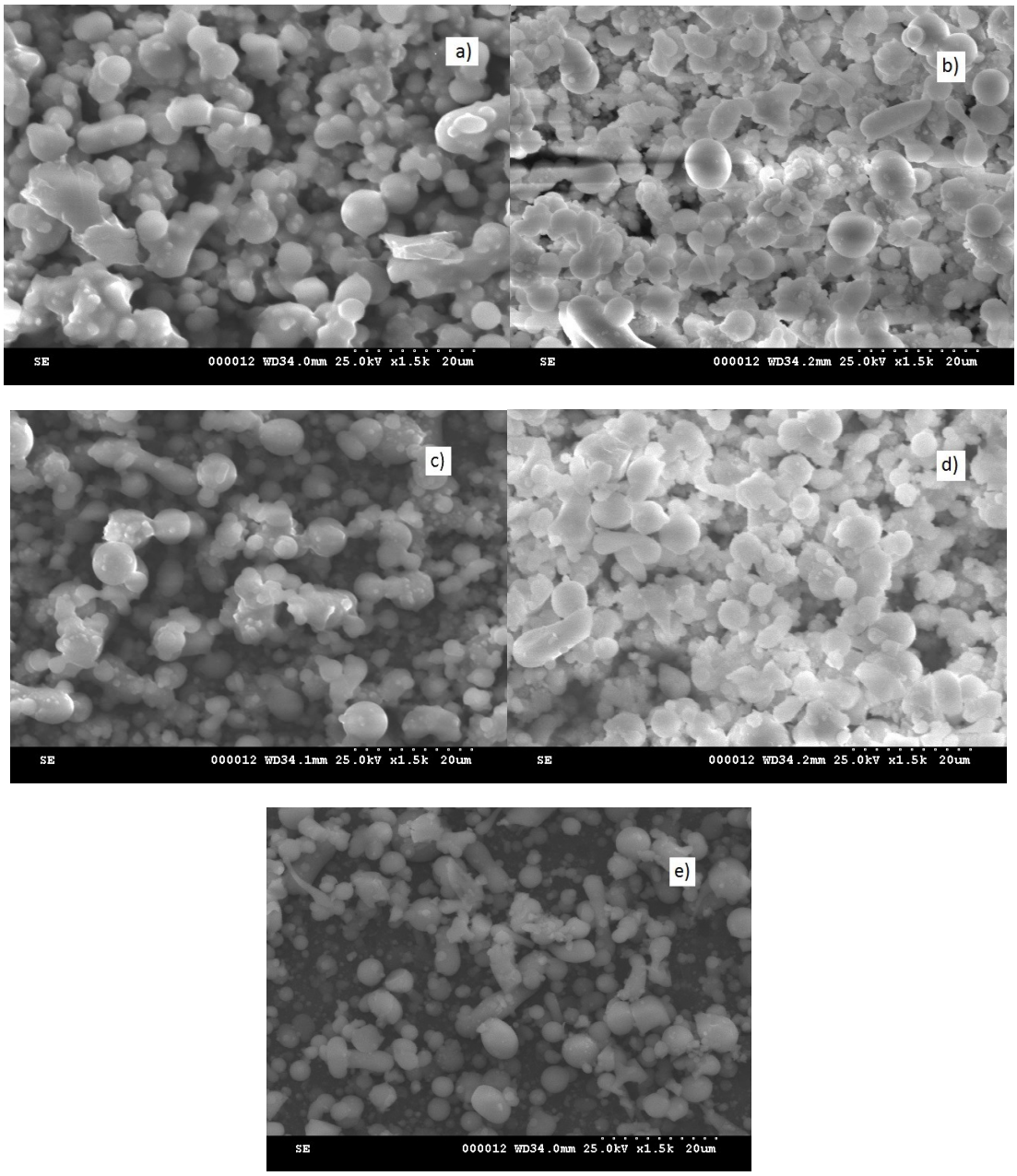

Fig. 4. SEM images for the films from a) experiment 1, b) experiment 2, c) experiment 3, d) experiment 4 and e) experiment 5.

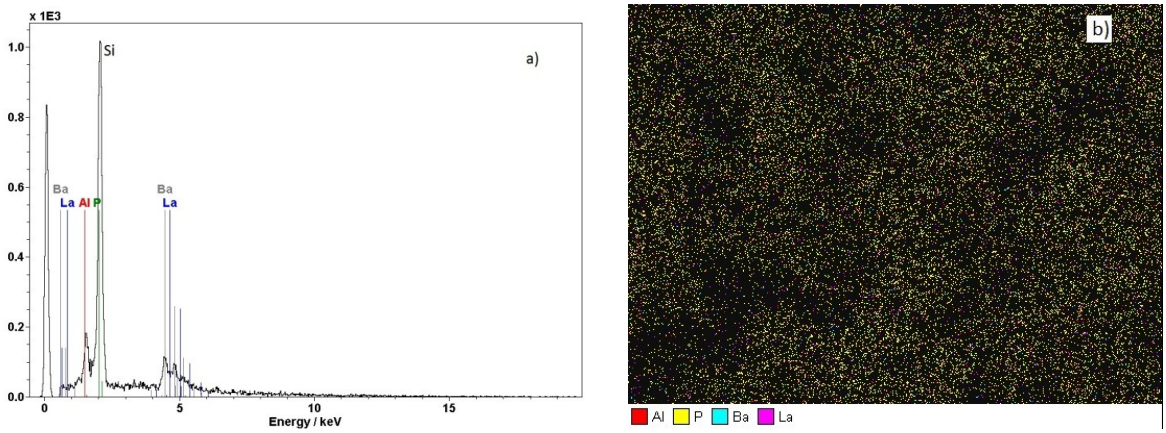

Fig. 5. a) EDX spectrum and b) elemental mapping of Al, P, Ba and La for the film from experiment 2.

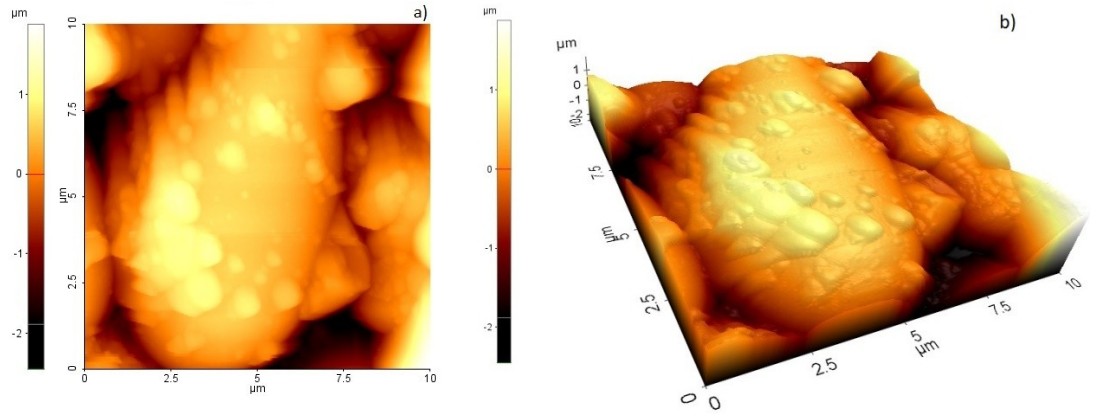

Fig. 6. a) 2D and b) 3D AFM images for the film from experiment 2.

The formation of the films from overlapped droplets is probably due to 248 nm wavelength used in the ablation process. These deposited films reveal a low smoothness surface of the film, as it is seen in the AFM images (Fig. 6).

4. Conclusions

Nd-doped phosphate films were prepared by PLD changing the pressure in the deposition chamber and the substrate temperature during the ablation process. The specific absorption bands in visible domain demonstrate the presence of Nd ions in the phosphate matrix. Raman and FTIR spectra of the PLD films detected vibrational bands related to the phosphate glass host.

SEM images showed that the reduction of the laser energy provided a poor uniformity of the deposited film due to the decreasing of the ablation rate. The increasing of the oxygen pressure in the vacuum chamber results in a decreasing of the uniformity and compactness of the film. Thus, a good uniformity and compactness of the deposited films is performed using a heated substrate and high vacuum.

Acknowledgments

This work was supported by a grant of the Romanian National Authority for Scientific Research, CNCS – UEFISCDI, project MNT-ERA.NET, contract No. 7-031/2011 and 186/2012 Partnership Program Project.

References

[1] J. E. Pemberton, L. Latifzahed, Chem. Mater **3**, 195 (1991).
[2] I. Belharouak, C. Parent, B. Tanguy, G. Le Flem, M. Couzi, J. Non. Cryst. Solids **244**, 238 (1999).
[3] J. E. Garbarczyk, P. Machowski, M. Wasiucionek, L. Tykarski, R. Bacewicz, A. Aleksiejuk, Solid State Ionics **136–137**, 1077 (2000).
[4] M. E. Jabotinski, Leningrad 35 (1980).
[5] A. Suarez-Garcia, R. Serna, M. Jiménez de Castro, C. N. Afonso, E-MRS Spring Meeting 2003 Symposium J-Rare Earth Doped Materials For Photonics, **2**, 17 (2003).
[6] W. A. Weyl, Coloured Glasses, London 77 (1976).
[7] T. Li, Proceedings of the IEEE **81**, 1568 (1993).
[8] S. Jiang, T. Luo, B. C. Hwang, F. Smekatala, K. Seneschal, J. Lucas, N. Peyghambarian, J. Non-Cryst. Solids **263–264**, 364 (2000).
[9] M. P. Bendett, N. A. Sanford, D. L. Veasey, US Patent 490748 (2005).
[10] G. Jose, G. Sorbello, S. Taccheo, E. Cianci, V. Foglietti, P. Laporta, J. Non-Cryst. Solids **322**, 256 (2003).
[11] M. Elisa, B. A. Sava, A. Diaconu, D. Ursu, R. Patrascu, J. Non-Cryst. Solids **355**, 1877 (2009).
[12] M. Elisa, B. A. Sava, A. Diaconu, L. Boroica, D. Ursu, I. Stamatin, F. Nastase, C. Nastase, Glass Phys. Chem. **35**, 596 (2009).
[13] J. D. Myers, R. Wu, G. M. Bishop, D. L. Rhonehouse, M. J. Myers, S. J. Hamlin, SPIE proc. **2379**, Shibin Jiang, 1995.
[14] B. I. Galagan, I. N. Glushchenko, B. I. Denker, Yu. A. Kalachev, N. V. Kuleshov, V. A. Mikhailov, S. E. Sverchkov, I. A. Shcherbakov, Kvant. Elektron. **39**, 1117 (2009).
[15] D. Barbier, X. Orignac, X. M. Du, R. M. Almeida, Sol–Gel Sci. Technol. **8**, 1013 (1997).
[16] X. Orignac, D. Barbier, X. M. Du, R. Almeida, Appl. Phys. Lett. **69**, 895 (1996).
[17] C. N. Afonso, Insulating Materials for Optoelectronics, edited by F. Agulló-López, World Scientific, Singapore (1995), Chap. 1, p. 1.
[18] R. Serna, J. M. Ballesteros, M. Jiménez de Castro, J. Solis, C. N. Afonso, Appl. Phys. **84**, 2352 (1998).

[19] M. Elisa, I. C. Vasiliu, C. E. A. Grigorescu, B. Grigoras, H. Niciu, D. Niciu, A. Meghea, N. Iftimie, M. Giurginca, H. J. Trodahl, M. Dalley, Opt. Mater. **28**, 621 (2006).
[20] C. Vasiliu, G. Epurescu, C. Grigorescu, M. Elisa, G. Pavelescu, A. Purice, A. Moldovan, M. Dinescu, Appl. Surface Sci. **253,** 8278 (2007).
[21] C. Vasiliu, G. Epurescu, H. Niciu, O. Dumitrescu, C. Negrila, M. Elisa, M. Filipescu, M. Dinescu, C.E.A. Grigorescu, J. Mater. Sci.: Mater. Electron., 1 (2008).
[22] E. M. Vogel, E. W. Chase, J. L. Jackel, B. J. Wilkens, Appl. Opt. **28**, 649 (1989).
[23] K. E. Youden, T. Gravatt, R. W. Eason, H. N. Rutt, R. S. Deol, G. Wylangowski, Appl. Phys. Lett. **63**, 1061 (1993).
[24] R. Serna, C. N. Afonso, Appl. Phys. Lett. **69**, 1541 (1996).
[25] J. C. G. de Sande, C. N. Afonso, J. L. Escudero, R. Serna, F. Catalina, E. Bernabeu, Appl. Opt. **31**, 6133 (1992).
[26] J. Gonzalo, F. Vega, C. N. Afonso, Thin Solid Films **241**, 96 (1994).
[27] Y. K. Sharma, R. P. Dubedi, V. Joshi, K. B. Karnataka, S. S. L. Surana, J. Eng. Mater. Sci. **12**, 65 (2005).
[28] J. Koo, B. S. Bae, H. K. Na, J. Non-Cryst. Solids **212**, 173 (1997).
[29] Y. Li, B. Ashton, St. D. Jackson, Optics Express **13**, 1172 (2005).
[30] Y. M. Lai, X. F. Liang, S. Y. Yang, J. X. Wang, L. H. Cao, B. Dai, J. Molec. Struct. **992**, 84 (2011).
[31] R. K. Brows, R. J. Kirkpatrick, G. Turner, J. Am. Ceram. Soc. **73**, 293 (1990).
[32] M. Elisa, B. A. Sava, I. C. Vasiliu, R. C. C. Monteiro, J. P. Veiga, L. Ghervase, I. Feraru, R. Iordanescu, J. Non-Cryst. Solids **369**, 55 (2013).
[33] D. Muresan, M. Dragan Bularda, C. Popa, L. Baia, S. Simon, Rom. Journ. Phys. **51**, 231 (2006)

*Corresponding author: feraru_i@yahoo.com